

Early Career Scientist Forum 2022 (Hybrid)

Location: Building 36, Rm. C211



October 25th, 26th, 27th

Organized by the *Science Director's Committee*

Organizing committee: Chris Bard (673), Mike Croteau (61A), Amir Ibrahim (616), Erika Kohler (691), Xiang Li (699), Melissa Ugelow (693)

Program Overview

The Early Career Scientist Forum is typically a 1-day AGU style conference for our scientists. Due to the nature of telework, the sessions have been broken into a 3-day agenda to add as much flexibility as possible and help facilitate attendance. Each day's session will be in person and hosted in a *Microsoft Teams* session. Any contractor, civil servant, postdoc, university-affiliated scientist, visiting scientist, or graduate student from the Sciences and Exploration Directorate (Code 600) can present, and everyone is invited to attend. ***The objective is to provide a chance for early career scientists*** to showcase their work, get feedback from other scientists, get to know their peers and to promote future collaboration.

Oral Presentations: Individual talks are 12 minutes long (+ 3 minutes for questions) and will begin promptly at their assigned time. The link to the Oral session is below the block schedule.

Any questions or difficulties connecting can be addressed at the [ECSF Helpdesk Team](#)

We hope you enjoy the sessions from all four SED Divisions!

Forum Schedule

Tuesday, October 25th			
Time	Presenter	Division	Title
9:00 AM	Christa D. Peters-Lidard	Director, Sciences and Exploration Directorate	Opening Remarks
Oral Session 1			
Session Chair: TBD			
Time	Presenter	Division	Title
9:15 AM	Christopher DiLullo	Astrophysics	Observing the Global 21 cm Cosmic Dawn Signal with the Long Wavelength Array
9:30 AM	Jenna Cann	Astrophysics	The X-ray properties of Low Metallicity Dwarf Galaxies
9:45 AM	Sambid Wasti	Astrophysics	ComPair : A Compton and Pair-Production telescope
10:00 AM	Travis Berger	Astrophysics	A First Look at the Homogeneously Characterized Kepler+K2+TESS Host Star and Planet Samples
15-min break			
Oral Session 2			
Session Chair: TBD			
Time	Presenter	Division	Title
10:30 AM	Noah Tuchow	Astrophysics	The Abundance of Belatedly Habitable Planets and Ambiguities in Definitions of the Continuously Habitable Zone
10:45 AM	John Ahlers	Astrophysics	Fascinating Worlds Around High-Mass Stars
11:00 AM	Michele L. Silverstein	Astrophysics	Exoplanet System Trends at the M Dwarf Convective Boundary
11:15 AM	Thomas Fauchez (V)	Planetary Science	CUISINES of the Worlds
11:30 AM	Vincent Kofman	Planetary Science	Noise simulations of exoplanet observations for transit and coronagraphic studies using the Planetary Spectrum Generator

Wednesday, October 26th**Oral Session 3****Session Chair: TBD**

Time	Presenter	Division	Title
8:30 AM	Pamela Wales	Earth Science	Developing a continuous ozone record through the SAGE and Aura missions with NASA reanalysis products
8:45 AM	Patrick Stegmann	Earth Science	The CRTM Coefficient Generation Package, Version 1.1
9:00 AM	Woubet G. Alemu (V)	Earth Science	An ensemble of Convolutional Neural Networks for Land Use Land Cover Classification in Northwest Ethiopia
9:15 AM	Kyle Gwartz	Earth Science	Data assimilation and the geodynamo: combining observations and dynamic models to understand the Earth's deep interior
9:30 AM	Ian Carroll (V)	Earth Science	Machine Learning Approaches for Predicting Phytoplankton Community Composition from simulated Ocean Color

15-min break**Oral Session 4****Session Chair: TBD**

Time	Presenter	Division	Title
10:00 AM	Morgaine Mckibben	Earth Science	Testing a hyperspectral, bio-optical approach for identification of phytoplankton groups in the Chesapeake Bay
10:15 AM	Charles Helms	Earth Science	Understanding the Vertical Slope of Snow Bands using Airborne Radar
10:30 AM	Ryan Kramer	Earth Science	The Opposing Roles of Radiative Feedbacks and Radiative Forcing in Driving Observed Precipitation Change
10:45 AM	Andrew Feldman	Earth Science	Observed Global Photosynthesis Response to Changing Rainfall Frequency and Intensity
11:00 AM	Kathleen McKee	Earth Science	Insights into the 15 January 2022 Hunga volcano, Tonga eruption using infrasound, lightning, and particle properties
11:15 AM	Niko Fedkin	Earth Science	Quantifying Oil and Natural Gas NO ₂ Sources over the Gulf of Mexico with Ship- and Satellite-based Data

15-min break**Oral Session 5****Session Chair: TBD**

Time	Presenter	Division	Title
11:45 AM	Ibrahim Mohammed (V)	Earth Science	Assessment of water resources conservation and sustainable management strategies in the Lower Mekong River Basin
12:00 PM	Nishan Kumar Biswas	Earth Science	Human impact and climate change in Bangladesh: understanding the stress on water resources from satellite

12:15 PM	Timothy M. Lahmers	Earth Science	The Role of Multivariate Data Assimilation in Characterizing Land Surface Response to Flood Events: A Case Study
12:30 PM	Manh-Hung Le (V)	Earth Science	An analysis of the transfer learning approach in predicting crop yield in the CONUS
12:45 PM	Tasnuva Rouf	Earth Science	Utility of satellite-based soil moisture in improving crop yield forecasting over agricultural zones in Argentina

Thursday, October 27th

Oral Session 6

Session Chair: TBD

Time	Presenter	Division	Title
9:00 AM	Rohit Chhiber	Heliophysics	An Extended and Fragmented Alfvén Zone in the Young Solar Wind
9:15 AM	Graham Kerr	Heliophysics	Diagnosing Suprathermal Protons via the Lyman Lines in Solar Flares
9:30 AM	Sanchita Pal	Heliophysics	On the erosion of large-scale solar magnetic flux ropes in the heliosphere
9:45 AM	Norberto Romanelli	Planetary Science	Solar Wind Turbulence Around Mars
10:00 AM	Michael Thorpe	Planetary Science	Unraveling the Sedimentary Rock Record of Mars with Terrestrial Analogs; Preliminary Results from the DIGMARS Project
10:15 AM	Vishnu Viswanathan	Planetary Science	Small Impact Craters Steered the Moon's Pole Along the Earth-Moon Direction

15-min break

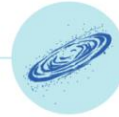
Oral Session 7

Session Chair: TBD

Time	Presenter	Division	Title
10:45 AM	Casey I Honniball	Planetary Science	The end of an era, the beginning of a legacy: SOFIA 6 μm VIPER observations
11:00 AM	Sourabh Shubham	Planetary Science	Moon Rocks - Predicting lunar rock types with geochemical data using machine learning tools
11:15 AM	Nathan Roth	Planetary Science	Composition of Comet C/2017 K2 Beyond the Water Sublimation Zone: ALMA Imaging of CO, HCN, H ₂ CO, and Cold CH ₃ OH
11:30 AM	Olivia Wilkins	Planetary Science	Structure-Specific Identification of Products Sublimated from UV-Photolyzed Cosmic Ice Analogues
11:45 AM	Svetlana Shkolyar	Planetary Science	Life Detection Knowledge Base: Organizing Astrobiology Knowledge for Mission Development and Calling for Contributors
12:00 PM	J. Blake Clark	Earth Science	The Transformation and Export of Organic Carbon Across an Arctic River-Delta-Ocean Continuum

(V): Virtual talk

Oral Session 1 - Tuesday 10/25



O101: Observing the Global 21 cm Cosmic Dawn Signal with the Long Wavelength Array

Christopher DiLullo (665)

The detection of the redshifted spectral signature from neutral hydrogen present during the formation of the first stars is a major goal in observational cosmology. The signal contains a trove of information which can place tight constraints on the astrophysical conditions under which the first stars form and evolve. The Experiment to Detect the Global EoR Signature (EDGES) collaboration reported a potential detection in 2018 which has both nonstandard amplitude and spectral shape. If this detection is validated, it would imply that current models of the early Universe need to be updated. I will present work that is part of an ongoing effort to validate the EDGES result using the Long Wavelength Array (LWA) in New Mexico. The LWA is a low frequency radio array which offers improved sensitivity via beamforming, a technique novel to the search for the global 21 cm signal.

O102: The X-ray properties of Low Metallicity Dwarf Galaxies

Jenna Cann (662) and Kim Weaver (662)

One of the primary outstanding questions in active galactic nuclei (AGN) astrophysics is the formation and early evolution of the supermassive black holes that are seen in nearly every massive galaxy. While theoretical simulations of various seed models have provided insight into the observational evidence needed to place constraints on the most probable formation pathway, current studies have primarily focused on AGNs in redder, bulge-dominated dwarf galaxies. This is a severe limitation, as the use of dwarf galaxies to probe seed black holes assumes a quiet cosmic history. This assumption may not be true of redder galaxies that have been affected by external factors, such as merging or tidal stirring, which would drive gas to the center, fueling star formation, enriching the gas, and potentially fueling the black hole. Therefore, only the study of IMBHs in local analogs of the pristine early galaxies, specifically low metallicity dwarf galaxies, can recover this vital missing link. These galaxies, however, are not typically as well-studied in the context of AGN science when compared to their higher metallicity and higher mass counterparts, and therefore require more detailed analysis to determine the efficacy of various diagnostics in uncovering AGNs in this population. In this presentation, I will present an analysis of the X-ray emission from local low metallicity dwarf galaxies, the truest local analogs

of the earliest galaxies that hosted the first seed black holes, and speak to the promise of current and future observatories in this space.

O103: ComPair : A Compton and Pair-Production telescope.

Sambid Wasti (661)

ComPair, a prototype of the All-sky Medium Energy Gamma-ray Observatory (AMEGO), is a balloon-borne project that is currently under development. AMEGO is a probe class mission concept designed to explore the MeV sky. At the medium energy of ~ 0.2 MeV to ~ 10 GeV, two processes compete for the photon interaction in matter. Compton scattering is dominant in the lower energies and pair production is dominant in the higher energies with the crossover around 10 MeV. AMEGO will be optimized for using both Compton and pair production to detect photons for a continuum sensitivity across a broad energy range. It consists of four major subsystems: Silicon tracker to measure the position and energy of the photon moving through the tracker layers, Cadmium-Zinc-Telluride (CZT) calorimeter to detect the Compton scattered photons, Cesium Iodide (CsI) calorimeter for measuring the high energy pair events and a plastic anti-coincidence detector to reject (veto out) charged particles. The prototype ComPair is being built to advance and validate the hardware and software tools used in AMEGO and uses the same four subsystems on a smaller scale. ComPair went through a beam-test at the Triangle Universities Nuclear Laboratory (TUNL) in late April of 2022 at Duke University. The two accelerator-based facilities, Free-Electron Laser (FEL) and the High Intensity Gamma-ray Source (HIGS) are designed to generate high energy photons that are carefully redirected towards our instruments. This allowed us to test our instruments in a high energy environment, similar to the environment for balloon altitude, which cannot be done in the typical laboratory. ComPair was exposed to various different energies from 2 MeV to 25 MeV. The beam was operated during the day and the test spanned for four days. The beam test served to validate and improve our calibration and also validate instrument integration. The beam data is being analyzed and the instruments are being optimized, tuned and updated in preparation for the balloon campaign in the fall of 2023. This talk will introduce the ComPair experiment and its instruments, review the beam test and present some results.

O104: A First Look at the Homogeneously Characterized Kepler+K2+TESS Host Star and Planet Samples

Travis Berger (667), Joshua Schlieder (667), Daniel Huber (University of Hawaii), Tom Barclay (667)

The wide availability of Gaia parallaxes and photometry has enabled homogeneous explorations of the physical properties of thousands of stars and exoplanets with exquisite precision and accuracy. Previously, such high-precision investigations were limited to hundreds of stars and planets, which were frequently dominated by inhomogeneities in the methods used to determine

their properties. By combining Gaia DR3 parallaxes, Bp and Rp photometry, and metallicities with an empirically calibrated PARSEC model grid, I will present the first homogeneous determination of physical properties for ~7900 Kepler, K2, and TESS host stars. In addition, I will present the resulting Kepler+K2+TESS planet population and highlight differences between the individual mission planet samples in planet radius - incident flux space. Finally, I will analyze the planet radius valley in three dimensions and comment on its implications for small planet formation and the relative likelihood of core-powered mass-loss and photoevaporation.

Oral Session 2 - Tuesday 10/25



O201: The Abundance of Belatedly Habitable Planets and Ambiguities in Definitions of the Continuously Habitable Zone

Noah Tuchow (667), Jason Wright (Penn State University)

A planet's history dictates its current potential to host habitable conditions and life. The concept of the Continuously Habitable Zone (CHZ) has been used to define the region around a star most likely to host planets with long-term habitability. However, definitions of the CHZ vary in the literature and often conflict with each other. Calculating the fraction of habitable zone planets in the CHZ as a function of stellar properties, we find that the quality of a star as a host for planets with long-term habitability and biosignatures depends strongly on the formulation of the CHZ used. For instance, older M stars are either excellent or sub-optimal hosts for CHZ planets, depending on whether one's definition of habitability prioritizes the total time spent in the habitable zone or the continuity of habitable conditions from the delivery of volatiles to its current age. In this study, we focus on Belatedly Habitable Zone (BHZ) planets, i.e. planets which enter the habitable zone after formation and volatile delivery due to the evolution of their host star. We find that between ~29-74% of planets in the habitable zone belong to this class of BHZ planets, depending on the timescale for the delivery of volatiles. Whether these planets can retain their volatiles and support habitable conditions is unclear. Since BHZ planets comprise a large portion of the planets we expect to survey for biosignatures with future missions, this open question of their habitability is an important factor for mission design, survey strategies, and the interpretation of results.

O202: Fascinating Worlds Around High-Mass Stars

John Ahlers (667), Knicole Colon (667), Ravi Kopparapu (699), Tom Barclay (667)

High-mass stars provide unique and fascinating environments for planets to form and evolve. The internal physics of A-type and F-type stars cause them to behave fundamentally differently than Sun-like and smaller stars, with traits such as rapid rotation, radiative exteriors, and a lack of external magnetic fields that produce dramatically different environments for orbiting planets. With nearly 40% of planets discovered to date orbiting A/F stars, it is more important than ever to understand how these stellar properties can impact planet formation and evolution. In this talk, I will give an overview of how high-mass stars differ from Sun-like stars as exoplanet hosts and discuss their implications for planet orbital evolution, atmospheric chemistry, and energy balance.

O203: Exoplanet System Trends at the M Dwarf Convective Boundary

Michele L. Silverstein (667), Joshua E. Schlieder (667), Thomas Barclay (667)

Using Gaia Data Release 2, Jao et al. (2018) identified an underdensity of stars marking the boundary between partially and fully convective M dwarfs. Low-mass stars in this "gap" feature of the HR diagram slowly expand and contract for up to billions of years, leading to luminosity changes, before settling as fully convective M dwarfs. Although a similar brightening of the Sun could send the Earth into a moist runaway greenhouse state, investigation is just beginning into the relationship between the unique history of gap M dwarfs and the formation and evolution of their planetary systems. To seek out defining system features in this recently discovered area of phase space, we obtain information on the stars and planets from the Gaia mission and the NASA Exoplanet Archive. We investigate key exoplanet system properties including radius, multiplicity, and period. Here we present the first results of our search for trends in these properties for several dozen confirmed exoplanets associated with the gap.

O204(V): CUISINES of the Worlds

Thomas Fauchez (693), Linda Sohl (611), Shawn-Domagal Goldman (693), Michael J. Way (611), Kostas Tsigradis (611), Ravi Kopparapu (699), Geronimo Villanueva (693), Vincent Kofman (693), Sara Fagi (693), Sandra Bastelberger (693), Jaime Crouse (693)

Model intercomparisons have been widely used for decades by the Earth science community. They are very valuable tools to improve models reliability, mitigate model dependencies, track down bugs and to provide benchmark for new models. Additionally, they provide the community

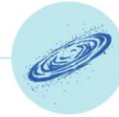
a way to assess and report the degree of consensus that exists between the models, and the associated uncertainties and origins of uncertainty that exist with respect to the conclusions drawn from the use of such models. In the era of James Webb Space Telescope, it becomes timely to focus community effort on benchmarking, comparing, and validating the performance of exoplanet models, both with respect to other models and to observations (when available). This is the objective of the Climates Using Interactive Suites of Intercomparisons Nested for Exoplanet Studies (CUISINES) NExSS Science Working Group. Within CUISINES exist several model intercomparisons for different kinds of model, such as CREME, CAMEMBER, MOCHA, SAMOSA, FILLET, PIE and MALBEC. In that presentation, I will review the content of all those tasty acronyms and why they are important for the exoplanet community. More info: <https://nexss.info/cuisines/>

O205: Noise simulations of exoplanet observations for transit and coronagraphic studies using the Planetary Spectrum Generator

Vincent Kofman (693), Geronimo L. Villanueva (693), Thomas J. Fauchez (693), Neil Zimmerman (667), Avi Mandell (693), Tyler Baines (667), Natasha Latouf (693),

Accurate noise simulations are necessary to determine the detectability of atmospheric features in exoplanets spectra and strategize for the most effective observations. Many aspects of the physical system have to be included to correctly budget the noise levels in a measurements, and detailed understanding of all of those aspects is required. From source to detector, noise components include the stellar and planetary source fluxes, including molecular, atomic, aerosols, and surface interactions with light, the contribution from zodiacal light, and the telescopes performance. In particular the telescopes performance consists of many components like the reflectivity of the different optical elements, the throughput of the used filters, as well as detector performance and noise, all of which are wavelength dependent and can be challenging to model. When considering coronagraph modeling, calculating the contrast and noise levels as a function of inner working angle and wavelength requires a detailed description of the optical effects within the instrument. The Planetary Spectrum Generator (PSG[1], psg.gsfc.nasa.gov/) contains all the elements to calculate the noise of spectroscopic observations. The noise simulator in PSG operates with a set of core parameters, which capture the performance of a telescope / instrument / detector combination. Figure 1 shows an overview of the parameters which are used to simulate the noise levels on space and ground-based observatories. The detectability of molecular features in exoplanet atmosphere depends strongly on the expected noise levels. We recently demonstrated the detectability of strong HDO features in an oxygen dominated TRAPPIST-1b atmosphere [2] using JWST/NIRSPEC and LUVOIR/HDI. Since that study, a number of steps have been made to further improve and quantify different noise sources. The better the different aspects of the noise are understood, the more we leverage this knowledge to maximize the scientific return of current and future space missions in planning astronomical observations. In this talk, the HDO case will be presented together with other examples to showcase the advanced abilities of the PSG in performing sensitivity studies and noise simulations for observations of transiting exoplanets and for exoplanet coronagraph studies.

Oral Session 3 - Wednesday 10/26



O301: Developing a continuous ozone record through the SAGE and Aura missions with NASA reanalysis products

Pamela Wales (610.1), K. Emma Knowland (610.1), Krzysztof Wargan (610.1), Brad Weir (610.1), Steven Pawson (610.1),

During the last quarter of the 20th century, the Stratospheric Aerosol and Gas Experiment (SAGE) missions were crucial in monitoring the loss and subsequent recovery of the stratospheric ozone layer. Due to the employed solar occultation and self-calibration method, the SAGE monitors have produced stable data throughout the lifetime of each instrument. However, over ten years passed between the end of the SAGE II and SAGE III/M3M missions in 2005 and the launch of SAGE III/ISS instrument in 2017, leaving a gap in the data that must be bridged in order to assess trends in the ozone record. The Modern-Era Retrospective analysis for Research and Applications, version 2 (MERRA-2) reanalysis product, with output available starting in 1980, is an attractive candidate for trend analysis due to the statistically optimized combination of multiple observing systems and the regular temporal and spatial coverage. However, changes in the assimilated observation systems can introduce discontinuities within the MERRA-2 ozone record, such as in 2004 when the MERRA-2 system shifted from assimilating ozone retrievals collected by SBUV instruments to those collected by instruments onboard the Aura satellite. In this study, we explore using the SAGE II record as a transfer function to develop a stable reanalysis data product, suitable for trend analysis, from the start of the SAGE II record in 1984 through the present. We follow the procedure outlined by Wargan et al. (2018) to address discontinuities in the MERRA-2 ozone dataset at the 2004 transition and during the Aura record. SAGE II ozone profiles are used to correct discontinuities in upper stratospheric ozone associated with changes in the MERRA-2 meteorological observing system in 1998 and 1995. We will then assess the relative performance of the data from different SAGE sensors using the resulting bias-corrected MERRA-2 ozone fields.

O302: The CRTM Coefficient Generation Package, Version 1.1

Patrick Stegmann (610.1), Benjamin Johnson (NOAA), Bryan Karpowicz (610.1), Isaac Moradi (610.1), Will McCarty (NASA-HQ)

The Community Radiative Transfer Model (CRTM) developed by the Joint Center for Satellite Data Assimilation (JCSDA) and applied by its partner agencies, NOAA, NASA, Navy, and Air

Force, is a fast, all-sky radiative transfer model for remote sensing and assimilation of observations in numerical weather prediction models. To this end, the CRTM needs to be able to perform radiance calculations that are both accurate and computationally very efficient. Additionally, tangent-linear (TL), adjoint (AD), and Jacobian/K-Matrix output is also required for different applications. One major factor that contributes to this goal is the efficient parameterization of the atmospheric gas transmittance for a very broad range of supported instruments. This includes MW, IR, hyperspectral IR, Visible, UV, and most recently also active sensors onboard satellites and airplanes. The process to obtain such a parameterization for each new instrument is complicated and involves the computation of a suitable training data with accurate first-principles line-by-line radiative transfer models, such as AERs LBLRTM and monoRTM. The dataset itself can be used as a basis for a variety of regression methods, such as the classical ODAS and ODPS algorithms, but also the newly developed CRTM-AI approach based on deep learning. The CRTM coefficient generation package strives to make the process more accessible to scientists at all partner agencies through the application of state-of-the-art software engineering, including agile development, Python interfaces, comprehensive documentation, and a modern build system.

O303(V): An ensemble of Convolutional Neural Networks for Land Use Land Cover Classification in Northwest Ethiopia

Woubet G. Alemu (618), Christopher N.R. Neigh (618), Jordan A. Caraballo-Vega (587), Margaret R. Wooten (618), Ejigu Muluken

Mapping areas with a complex topography and highly fragmented small-holder land use land cover (LULC) areas, such as the Amhara Region of Ethiopia, requires very high-resolution satellite imageries and robust classification methodologies. To this end, we have analyzed the pan-sharpened 2-meter very-high-resolution (VHR) WorldView multi-temporal imageries using Convolutional Neural Networks (CNNs). Training and test LULC class datasets were obtained from the Land Investment for Transformation (LIFT) Ethiopia project that was digitized from centimeter-level special mission aerial photos. Several CNNs were used for the task of semantic segmentation and compared their performance to other machine learning algorithms such as decision tree models. Extensive geometric data augmentation and pre-processing techniques were performed to account for the spectral distribution of landscape features in the imagery at different dates. We have classified the region into eight broad land cover classes that comprise cropland, grassland, shrubland, forest, bareland, settlement, water, and wetland. While both LULC classification methods achieve sufficient overall accuracies, CNNs outperform the Random Forest algorithm in classifying the LULC of the study area. With CNNs, we were able to classify small features and classes with small occurrences in the training dataset by taking into consideration spatial features and class weighting. These research outputs will be beneficial in making informed decisions by the Amhara Region government sectors, and non-governmental Index-Insurance organizations on food security, market management, and the crop insurance sector. We will use the cropland maps as a baseline for yield estimation and forecasting in our

subsequent research work, which in turn can be used for recurrent seasonal yield estimation and forecasting that are useful for planning purposes to alleviate food insecurity.

O304: Data assimilation and the geodynamo: combining observations and dynamic models to understand the Earth's deep interior

Kyle Gwirtz (61A), Weijia Kuang (61A)

The geodynamo is the system by which the Earth's intrinsic magnetic field is generated and sustained through fluid motion in the planet's electrically-conducting outer core. The turbulent core flow leads to a magnetic field which varies on a broad range of timescales. Over years to decades the detailed field structures can change, while on longer timescales of millennia, the (typically) dipole-dominated magnetic field can reverse polarity, i.e., switching the magnetic north and south poles. However, because the outer core is not directly observed, understanding and predicting these variations presents a major challenge. Over the last decade, significant interest has developed in applying data assimilation (DA) to the study of the geodynamo. Simply put, DA is a general term for methods which merge observations with dynamic models in order to estimate a system's state and forecast future behavior. In the study of the geodynamo, DA can be used to combine observations of the geomagnetic field with numerical dynamo models, to estimate the state of the outer core and forecast future variations. However, while DA has been successfully implemented in other Earth Science applications, the careful selection and tailoring of DA techniques to a particular problem are critical to making optimal use of available models and data. In the study of the geodynamo, significant work in determining optimal DA methodologies remains to be done before the full potential of DA in this setting can be realized. In this talk we review the developing application of DA to the study of the geodynamo, and discuss our recent work regarding the ability of DA to constrain the magnetic field and fluid flow in the Earth's deep interior.

O305(V): Machine Learning Approaches for Predicting Phytoplankton Community Composition from simulated Ocean Color

Ian Carroll (616), Susanne Craig (616), Cécile Rousseaux (616)

Demand for satellite-derived estimates of phytoplankton community composition (PCC), or the relative abundance of taxonomically resolved phytoplankton groups, has accelerated due to increasing recognition that PCC variation affects the uptake of atmospheric CO₂, how much of this photosynthetically fixed C sinks to the deep ocean over climate-relevant time scales, and how efficiently energy is transferred to higher trophic groups, including economically important fisheries species. The Plankton, Aerosol, Cloud, ocean Ecosystem (PACE) Mission envisions first-ever production of global PCC estimates derived from hyperspectral reflectances, to be collected by the Ocean Color Instrument (OCI). During the first PACE Science Team period, biogeochemical, radiation and circulation models (NASA Ocean Biogeochemical Model, Ocean-Atmosphere Spectral Irradiance Model and Poseidon respectively) were used in combination with the assimilation of existing, multi-spectral, satellite ocean color to model water leaving radiances that realistically simulate would-be observations by OCI. The data include densities of chlorophyll across four taxonomic groups of phytoplankton and corresponding normalized water-leaving radiances. An expanded version of the dataset, covering multiple years with daily temporal resolution, provides a sufficient number of pixel-level observations to quantify performance of machine learning algorithms in their estimation of PCC from ocean color. Two types of feed-forward neural networks are

compared using the Tensorflow modeling software: a multi-layer perceptron (MLP) and a convolutional neural network (CNN) with 1-d convolution over the 1 nm resolved spectrum. Despite the lack of regularization, neither model shows indications of over-fitting as divergence over epochs between losses calculated from the training and validation subsets. The CNN out-performs the MLP on the basis of total mean squared and absolute error on the test subset; however, none of the performance metrics in the Tensorflow package address error covariance. Each model is designed to predict four chlorophyll densities simultaneously, and ongoing work investigates customization of both the loss function used during optimization and the performance metrics to eliminate and assess (respectively) correlations in the model error. Future aims include a probabilistic model comparison based on the likelihood of the test data under posterior predictive distributions, assuming multivariate normal data with known means provided by the model and Inverse-Wishart distributed covariance estimated from the validation data.

Oral Session 4 - Wednesday 10/26



O401: Testing a hyperspectral, bio-optical approach for identification of phytoplankton groups in the Chesapeake Bay

Morgaine Mckibben(610), Stephanie Schollaert Uz (610), Sherry Palacios (CSU-Monterey Bay)

NASA's upcoming hyperspectral missions, such as Plankton Aerosol Cloud ocean Ecosystem (PACE) scheduled to launch in early 2024, will advance decades of ocean color observations from the multi- to hyperspectral domain. PACE's Ocean Color Imager (OCI) provides the greater spectral resolution necessary to deconvolve in-water constituents in optically complex coastal zones. For example, advancement of standard, multi-spectral-based estimates of chlorophyll-a concentration, a proxy of total phytoplankton community abundance, will enable discrimination of which phytoplankton groups comprise that total. In this work the theoretical framework of Phytoplankton Detection with Optics (PhyDOTax), a hyperspectral, bio-optical approach to differentiating phytoplankton taxonomic classes, is applied and evaluated in the Chesapeake Bay. Developed in the Monterey Bay of California, PhyDOTax includes a matrix-based decomposition algorithm that deconvolves the water's spectral signal into its component phytoplankton groups. In this project, PhyDOTax is regionally parameterized and validated in the Chesapeake Bay. Validation results show statistically significant performance when applied to synthetic data under certain conditions and reduced performance in others. Similarly, field evaluation shows algorithm skill at seasonal scales but variable performance at individual in situ stations. Results of efforts to improve this performance are discussed including: sensitivity analyses of influences by non-algal optical constituents (e.g. colored dissolved organic matter and sediment), testing varied spectral inputs, and lab-based parameterization efforts. The Chesapeake Bay estuary hosts diverse and economically important ecosystem services to the Mid-Atlantic United States that are changing due to anthropogenic pressures. Potential for this area of applied research in the context of Bay stakeholders' water quality monitoring and decision-making needs is also discussed.

O402: Understanding the Vertical Slope of Snow Bands using Airborne Radar

Charles Helms (612), Gerald M. Heymsfield (612), Stephen D. Nicholls (612)

Snow bands are frequently responsible for dumping large amounts of snow over a relatively small region and pose a considerable forecasting challenge. The ongoing NASA Investigation of Microphysics and Precipitation for Atlantic Coast-Threatening Snowstorms (IMPACTS) field campaign observed several instances of these snow bands during January and February of 2020 and 2022. These snow bands were sampled by a combination of airborne (NASA ER-2 and P-3) and ground-based remote sensing and in-situ instruments. Along-band cross sections of these snow bands reveal that many of them are vertically sloped. Our preliminary analysis into one of these snow bands suggests that the vertical slope is not maintained by large-scale thermodynamic forcing and does not appear to be tied to horizontal deformation wind patterns collecting the snow particles into banded features. A combined analysis of the radar reflectivity and wind retrievals from the ER-2 radars raises the possibility that these features could be produced by vertical wind shear layers deforming fall streaks into bands that extend hundreds of kilometers. The present study will focus on extending our preliminary analysis to additional cases and understanding the mechanisms that support these features using a combination of radar data, in-situ aircraft measurements, and numerical modeling.

O403: The Opposing Roles of Radiative Feedbacks and Radiative Forcing in Driving Observed Precipitation Change

Ryan Kramer (613), Daeho Jin (613), Lazaros Oreopoulos (613)

While there is clear evidence of extreme precipitation events increasing in frequency and intensity over the recent anthropogenically-forced historical period, the same cannot be said for total precipitation in the global-mean, which has not exhibited robust positive trends with recent global-warming, as theory predicts. In the global-mean, precipitation is largely controlled by atmospheric radiative cooling, which also does not have a clear trend in observations. Using satellite data from the GPCP, CERES, AIRS and CloudSat missions, we demonstrate that the lack of radiative cooling, and thus precipitation, trend is due to a cancellation between radiative feedbacks versus greenhouse gas radiative forcing, which acts to radiatively cool and radiatively heat the atmosphere, respectively. These results offer a new perspective for why climate models also simulate limited global-mean precipitation change over the historical record.

O404: Observed Global Photosynthesis Response to Changing Rainfall Frequency and Intensity

Andrew Feldman (618), Abhishek Chatterjee (JPL), Joanna Joiner (614), Benjamin Poulter (618)

Rain events are globally becoming more intense and less frequent under a changing climate. These intra-seasonal rainfall features have received less attention than changes in annual total rainfall and mean temperature in their influence on the global carbon cycle. However, field rainfall manipulation experiments show non-negligible (10%-20%) changes to annual gross primary production (GPP) in response to rainfall frequency alterations, while holding total annual rainfall constant. Nevertheless, field

and modeling experiments show little consensus on the sign change of annual GPP due to changing rainfall intensity and frequency. In this study we ask: based on satellite observations, how is global photosynthesis responding to changes in rainfall intensity and frequency? How and why do photosynthesis responses vary across drylands and humid biomes? Using OCO-2 solar induced fluorescence, MODIS normalized difference vegetation index, and SMAP vegetation optical depth retrievals, we isolate the average photosynthesis response to rainfall intensity and frequency with statistical techniques. We find that GPP in more humid ecosystems tends to respond negatively to years with more intense, less frequent rainfall, while dryland GPP does not show a consistent response to these changes. Mean annual soil moisture and VPD responses appear to drive GPP responses in humid ecosystems: more intense, less frequent rain tends to increase VPD and decrease soil moisture on average. However, dryland ecosystems are more sensitive to rainfall intensity and frequency, with typical interannual rainfall frequency variations altering annual GPP by 10%-20%. With increasing importance of pulse characteristics in drylands, strong vegetation pulse responses to individual rain events appear to reduce occurrence of negative GPP responses to more intense, less frequent rain. We ultimately find that rainfall intensity and frequency (beyond total annual rainfall) partially drive GPP interannual variability, especially in drylands. Additionally, based on initial assessments of rainfall trends, more intense, less frequent rainfall will likely decrease global annual GPP.

O405: Insights into the 15 January 2022 Hunga volcano, Tonga eruption using infrasound, lightning, and particle properties

Kathleen McKee (613), V.J.B. Flower, R.A. Kahn (613), J.D. Assink, C. Vagasky, S. Behnke, A. Van Eaton, L. Mastin, J.A. Limbacher (613), K.T. Junghenn Noyes (613)

We examine the 15 January 2022 eruptive episode of Hunga volcano, Tonga by combining infrasound from nearest International Monitoring System arrays, lightning, and Multiangle Imaging Spectroradiometer (MISR) data. Infrasound analysis suggests the eruption started between 3:50 and 3:57 UTC and had additional pulses, most notably one around 8:30 UTC. Lightning, which is linked to plume height and presence of ash, started after 4:00 UTC. MISR, aboard NASA's sun-synchronous Terra satellite, has a 380 km observational swath and provides a snapshot of aerosol characteristics: altitude, relative velocity, and microphysical properties. Microphysical characteristics (radius, sphericity, and light absorption) enable us to infer if particles are sulfate/water, ash (non-spherical, weakly to strongly absorbing), or ice for a volcanic plume. Analysis of the MISR observation at 22:05 UTC on 15 January shows an ash-rich plume at 10-14 km a.s.l., swath centerline ~330 km to the west of Hunga. Preliminary particle property analysis shows a decrease from 1-3 microns to ~0.5 micron ash particle radius with increasing distance from Hunga. The particle size difference in the MISR data could reflect changes in initial emission or plume evolution. We combine atmospheric wind and temperature profiles, GOES data, and NOAA HYSPLIT and Ash3D modeling to investigate the particles' time history, in order to relate particle characteristic changes to infrasound and lightning changes. HYSPLIT modeling suggests the particles were emplaced at least 15 km a.s.l, lower altitude winds were blowing to the east. Initial Ash3D results suggest the particles may have been part of the >30 km a.s.l. umbrella that then fell ~20 km in 15-20 hours, to the observed height at MISR overpass time. Thus, a considerable fallout rate would be necessary to have ash where MISR observed it, which would require a process beyond simple gravitational settling, such as ash aggregation or downward meteorological advection. Subsequent MISR retrievals of the plume downwind do not observe any ash particles supporting possible early deposition.

O406: Quantifying Oil and Natural Gas NO₂ Sources over the Gulf of Mexico with Ship- and Satellite-based Data

Niko Fedkin (614), Ryan Stauffer (614), Anne Thompson (614),
Debra Kollonige (614), Lok Lamsal (614)

The Gulf of Mexico (GOM) Outer Continental Shelf (OCS) is home to numerous oil and natural gas (ONG) production activities. These activities are a source of nitrogen dioxide (NO₂), a harmful trace gas produced through fuel combustion. Industry self-reported emissions of NO_x derived from fuel usage statistics provide the only current estimates for the distribution of ONG sources over the GOM. In-situ NO₂ data over the GOM are not routinely collected, making it difficult to monitor air quality in the region. A ten-day 2019 ship campaign, the Satellite Coastal and Oceanic Atmospheric Pollution Experiment (SCOAPE), was conducted by NASA in collaboration with the Bureau of Ocean Energy Management (BOEM), the agency responsible for ensuring that ONG activities do not significantly impact air quality of populated areas. SCOAPE confirmed that NO₂ data from both ground-based and satellite remote sensing instruments can track ONG emissions over the GOM. This work complements the brief SCOAPE snapshot by using satellite data to quantify seasonal and interannual variations in spatial NO₂ patterns over the GOM. We make use of 1) monthly OMI and TROPOMI NO₂ time series calculated over an 18-year period (2005-2022 for OMI; 2018-2022 for TROPOMI); 2) in-situ and remotely sensed data from the 2019 SCOAPE campaign to better characterize relationships between surface concentrations and satellite column amounts; (3) meteorological analysis using MERRA-2 reanalysis data and trajectories to assess the contributions of OCS and land NO₂ sources. These latter analyses will provide correlations between surface and satellite measurements and more refined assessments of how satellite data can be used to monitor NO₂ from ONG in a region where activity is expected to grow with new leases.

Oral Session 5 - Wednesday 10/26



O501(V): Assessment of water resources conservation and sustainable management strategies in the Lower Mekong River Basin

Ibrahim Mohammed (617), John D. Bolten (617), Nicholas J. Souter (Conservation International),
Kashif Shaad (Conservation International), Derek Vollmer (Conservation International)

Uncertainties and indeterminate scope, divergent social values and stakeholder interests, and changing hydroclimatology in transboundary river basins are all factors that may complicate sustainable water resource management. To address such complex socio hydrological issues, we present an example of an integrated approach to assessing future sustainability challenges in their social, hydrological, and

ecological dimensions using a case study from the Lower Mekong basin. Our study area here is the combined basin of the Se Kong, Se San, and Sre Pok (3S) rivers which deliver approximately 20% of flow to the Mekong River system. We used a mixed methods approach to analyze potential impacts of climate change on regional hydrology, the ability of dam operation rules to keep downstream flow within acceptable limits, and the present state of water governance in Laos, Vietnam, and Cambodia. Our results suggest that future river flows in the 3S river system could move closer to natural (i.e. pre-development) conditions during the dry season and experience increased floods during the wet season. This anticipated new flow regime in the 3S region would require a shift in the current dam operations, from maintaining minimum flows to reducing flood hazards. Moreover, our Governance and Stakeholders survey assessment results revealed that existing water governance systems in Laos, Vietnam, and Cambodia are ill-prepared to address such anticipated future water resource management problems. Our results indicate that the solution space for addressing these complex issues in the 3S river basins will be highly constrained unless major deficiencies in transboundary water governance, strategic planning, financial capacity, information sharing, and law enforcement are remedied in the next decade. This work is part of an ongoing research partnership between the National Aeronautical and Space Agency (NASA) and the Conservation International (CI) dedicated to improving natural resources assessment for conservation and sustainable management.

O502: Human impact and climate change in Bangladesh: understanding the stress on water resources from satellite

Nishan Kumar Biswas (617), Augusto Getirana (617), Sujay Kumar (617)

Bangladesh, a developing country striving to become a food-sufficient nation, is dealing with the demands of a population of more than 160 million people. To ensure optimized food production, the country has expanded the agricultural land to a great extent and increased the cropping frequency in recent decades. When the cropping frequency increased, the dry season crops depend on groundwater resources for the irrigation due to surface water scarcity. In this study, we characterize the agricultural expansion and its impacts on water resources using satellite and in situ datasets. The expansion of the cropland was quantified using the NASA MODIS satellite provided annual land cover dataset. From the in-situ groundwater table data, the trend was analyzed to identify the region of the country with the most negative trend. MODIS satellite provided Leaf Area Index (LAI) data was used to see the increasing trend in agricultural activity and a match was found with the groundwater table data trend. Using the NASA MODIS satellite provided evapotranspiration data, an increasing trend found in the region with dry season agriculture, which can be explained by the flooding irrigation practices. The GRACE satellite provided terrestrial water storage (TWS) data, which was used to quantify the impact of groundwater depletion on the TWS availability. The decreasing trend in precipitation over the country was also seen from the NASA GPM satellite. It was found that the decreasing trend in precipitation with the depletion of groundwater has already put an enormous stress on the water resources in the region which has impact on the drinking water availability, groundwater contamination, and saltwater intrusion. This study sheds light on the understudied relationship between the different phenomena, which will be useful in terms of identification of the water-stressed region, and future policy decisions.

O503: The Role of Multivariate Data Assimilation in Characterizing Land Surface Response to Flood Events – A Case Study

Timothy M. Lahmers (617), Sujay V. Kumar (617), Kim A. Locke (617), Shugong Wang (617), Augusto Getirana (617), Melissa L. Wrzesien (617), Pang-Wei Liu (617), Shahryar Khaliq Ahmad (617)

Hydrologic extremes, such as floods, have complex triggering processes, including rain, snowmelt, and antecedent soil moisture. Flood events can also have secondary impacts, such as changes to vegetation growth. To model a flood event and its impacts, these processes must be accurately represented. The 2019 Northern Mississippi Basin flood, which resulted in a series of hydrologic disturbances, is an example of this type of complex event. It began with anomalously high snow amounts during winter 2018-2019 and above-average spring precipitation. This series of anomalies resulted in higher than normal soil moisture that prevented crops from being planted over much of the corn belt region. In the present study, we demonstrate the need for data-assimilation (DA) of remote sensing products in a hydrologic modeling system to capture the processes that led to the 2019 flood event and the resulting agricultural impacts. DA is performed through the NASA Land Information System (LIS) modeling framework, where the Noah-MP land surface model and the HyMAP river routing scheme are coupled. We investigate where DA of AMSR2 snow depth retrievals, SMAP soil moisture, and MODIS LAI is necessary for the model to capture this sequence of hydrologic disturbances. We also consider the impacts of DA on HyMAP streamflow and water balance. Results show that DA of remote sensing products with the land surface model is needed to fully understand the chain of processes that caused the 2019 flood and its impacts. This is likely attributed to limitations in the Noah-MP schemes for snowmelt, vertical soil processes, and vegetation. This case study from a high impact event demonstrates the ability of DA to resolve human caused processes, such as agriculture, and the need for continued investment in remote sensing observations.

O504(V): An analysis of the transfer learning approach in predicting crop yield in the CONUS

Manh-Hung Le (617/ SAIC), Tasnuva Rouf (617/ SAIC), John Bolten (617)

Regional and national crop yields are fundamental agricultural statistics that provide insight into season-ending production. The use of remotely sensed datasets (e.g., NDVI, soil moisture) is a promising method for predicting crop yields at large scales. To develop this method, historical relationships between remotely sensed datasets and crop yield observations are used. Long-recorded yield statistics are a fundamental requirement for the model accuracy. Many agricultural regions, however, lack long-term yield records. This limits the geographical application of the satellite-based crop yield model. This study proposes transfer learning as a method for improving these models in geographical yield modeling extrapolation. Transfer learning is an area of research in the field of machine learning. It addresses using information from one problem, i.e., the source, to improve the performance of a model on another problem, i.e., the target. In this experiment, we will employ the transfer learning concept in modelling corn and soybean yields across the CONUS. We selected several counties having long-term record crop yield data as the source. At the source, we train different satellite-based crop yield models and then transfer these models to other counties (the target), where we assume the data is pseudo limited. We test the ability of models trained on data from the source by comparing these models with benchmark models

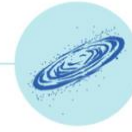
at the target. The results of this study can be applied to monitoring and forecasting crop yields in regions with limited data availability through satellite-based models.

O505: Quantifying Oil and Natural Gas NO₂ Sources over the Gulf of Mexico with Ship- and Satellite-based Data

Tasnuva Rouf (617/SAIC), Manh-Hung Le (617/SAIC), John Bolten (617)

Accurate and timely forecasting of crop yields is crucial to the sustainable development of agriculture and global food security. Crop models are used to forecast major crops in several regions of the world. However, these models are computationally expensive and difficult to scale as they require large sets of data and are difficult to calibrate effectively for various regions of the world. Approaches utilizing remotely sensed data, potentially provide a relatively easier, more effective alternative. This work proposed forecasts the crop yields of three major crops (corn, soybean, and winter wheat) over major growing agricultural zones in Argentina using vegetation indices and a well-established lag relationship of near-surface soil moisture. Previous studies have mainly focused on developing forecasting models for a specific crop type and location using a single source of data (e.g., vegetation indices), thus providing little insight into the forecasting models' performance on different crop types and regions. Since satellite-based soil moisture is a critical indicator of agricultural yield and exhibits a significant lag correlation with NDVI, this study aims to improve crop yield forecasting by incorporating operational satellite-based SMAP and NDVI data. First, we employed an area under the NDVI curve versus crop yield model for major crop-growing in the study domain. Then, we developed the SMAP-based Dynamic Agricultural Productivity Indicator (DAPI) by combining SMAP and NDVI data to improve the NDVI and crop yield forecasting methods. Our proposed method performed differently for different crop types and regions, with soybeans performing better than corn. In general, the performance of the NDVI forecasting models decreases with increasing lead-time, with a one-month lead-time yielding the best model performance. Furthermore, DAPI outperformed to estimate the expected NDVI response more accurately than the default method in most case study regions. This study will be a foundation for developing a methodology using remote sensing data for forecasting global agricultural productivity.

Oral Session 6 - Thursday 10/27



O601: An Extended and Fragmented Zone in the Young Solar Wind

Rohit Chhiber (671), William Matthaeus, Arcadi Usmanov (673), Riddhi Bandyopadhyay, Melvyn Goldstein, Steven Cranmer

The transition from the magnetically structured solar corona into the increasingly hydrodynamic solar wind is believed to occur across the so-called Alfvén radius, or Alfvén surface. Motivated by theoretical, numerical, and observational evidence, we investigate the influence of solar-wind turbulence on this surface, which leads to the possibility that the critical transition between sub-Alfvénic flow and super-Alfvénic flow takes place in fragmented and disconnected subvolumes within a general Alfvén critical zone. We use a global magnetohydrodynamic model of the solar wind, coupled to a turbulence transport model, to generate possible realizations of such an Alfvén zone. Understanding this transition will inform theories of coronal heating, solar wind origin, solar angular momentum loss, and related physical processes in stellar winds beyond the Sun.

O602: Diagnosing Suprathermal Protons via the Lyman Lines in Solar Flares

Graham Kerr (671) and Joel Allred (671)

Particle acceleration is a ubiquitous process in the Universe, but is not well understood. During solar and stellar flares, the prevailing view (supported by a substantial body of evidence) is that energy is transported through the solar/stellar atmosphere by beams of non-thermal electrons, accelerated following magnetic reconnection. This makes them ideal laboratories to study particle acceleration. Models of particle acceleration also predict the acceleration of protons or heavier ions. However, due to the lack of constraints on their properties they are largely ignored in solar and stellar models. This is despite the fact that they carry energy equivalent to the electrons. Said in another way: we may be ignoring up to half of the energy transported during flares. To address this we have been running models of proton-beam driven solar flares, and from those making predictions of how they may be detected using the hydrogen UV Lyman lines. Suprathermal protons may charge exchange with chromospheric neutral hydrogen, creating energetic natural atoms. These ENAs may subsequently emit a highly Doppler shifted photon, so that broad features may appear in the wings of the Lyman lines. We demonstrate that, while a tricky observation, these should be observable by instruments such as Solar Orbiter's SPICE.

O603: On the erosion of large-scale solar magnetic flux ropes in the heliosphere

Sanchita Pal (672), Soumyaranjan Dash, Emilia Kilpua, Dibyendu Nandi, Simon Good, Jens Pomoell, Daniel J Price

Large-scale solar magnetic flux ropes (MFRs) in the interplanetary medium may have significant space weather impacts. Their geoeffectiveness depends on their properties that evolve during the interplanetary passage. Based on analysis of observations obtained from spacecraft at different heliocentric distances, we show that MFRs interacting with the draped ambient solar wind magnetic field lose a substantial amount of their initial magnetic flux via magnetic reconnection and this eroded flux has linear correlation with the solar open flux that majorly shape the heliosphere. The solar open flux is governed by the sunspot cycle; therefore, we uncover a hitherto unknown pathway for solar cycle modulation of MFR properties. We study the influence of erosion on MFRs and find that MFR erosion significantly impacts their geoeffectiveness. It can peel off MFR's highly twisted envelop created during their formation at low corona. It can significantly impact MFR's inherent magnetic properties and affect their flux and helicity budgets in the heliosphere. Our study has significant implications for understanding MFR evolution governed by erosion.

O604: Solar Wind Turbulence Around Mars

Norberto Romanelli (695) and Gina A. DiBraccio (670)

We present a statistical analysis on the variability of the incompressible energy cascade rate in the solar wind around Mars, making use of an exact relation for fully developed turbulence and more than five years of Mars Atmosphere and Volatile Evolution (MAVEN) observations. Using magnetic field and plasma data, we compute the energy cascade rate at the Magnetohydrodynamics (MHD) scales in the pristine solar wind. From our statistical results, we conclude that the incompressible energy cascade rate decreases as the Martian heliocentric distance increases, for each of the three explored Martian years. Moreover, we suggest that the presence of proton cyclotron waves, associated with the extended Martian hydrogen exosphere, do not have a significant effect on the nonlinear cascade of energy at the MHD scales.

O605: Unraveling the Sedimentary Rock Record of Mars with Terrestrial Analogs; Preliminary Results from the DIGMARS Project

Michael Thorpe (699)

Preserved in the sedimentary rocks of Mars is a rich record of ancient river and lake environments accompanied by surficial weathering and subsurface diagenetic conditions. The Digging Iceland Geology for Mars Analog Research Science (DIGMARS) project aims to provide a terrestrial reference frame for these sedimentary rocks, exploring groundwater-sediment interaction from lakes around Iceland. Here, we present a preview of our 2021 and 2022 field campaigns to Iceland as well as initial results from our laboratory analysis of aqueous and sediment samples. When this terrestrial reference frame is applied to regions of Mars (e.g., Gale crater), it becomes clear how early diagenesis from sediments interacting with percolating groundwaters could have a profound impact on interpretations of the sedimentary history of lacustrine environments.

O606: Small Impact Craters Steered the Moon's Pole Along the Earth-Moon Direction

Vishnu Viswanathan (698), Erwan Mazarico (698), Sander Goossens (698), David E. Smith (MIT), James W. Head (Brown), Gregory Neumann (698), Maria Zuber (MIT)

The Moon preserves most of its ~4.5 billion year surface bombardment history, visible through its present-day gravity field and topography datasets, recovered from the GRAIL and LRO missions, respectively. Any change to the distribution of mass, e.g., from a cratering event, influences the minimum (rotational) energy orientation of the Moon, subsequently causing a change in its secular orientation with respect to its rotational axis – a phenomenon known as True Polar Wander (TPW). Large craters, fewer in number, left large gravitational contributions (called anomalies), while smaller craters, more numerous, contributed to small individual gravitational anomalies. Here we show that the cumulative effect of the small craters had a significant contribution to the Moon's degree-2 shape, and its asymmetric distribution steered the overall polar wander of the Moon along the direction of the Earth-Moon tidal axis. This reorientation places the near-side Procellarum region ~10° higher in latitude in the past, placing the Th-rich deposits and their antipode closer to the poles. An article detailing this work was recently accepted for publication in the Planetary Science Journal.

Oral Session 7 - Thursday 10/27



O701: The end of an era, the beginning of a legacy: SOFIA 6 μm VIPER observations

Casey I Honniball (698), William T. Reach, Paul G. Lucey, Anicia Arredondo, and Eric R. Malaret

Introduction: The conclusion of the Stratospheric Observatory For Infrared Astronomy (SOFIA) brings the end of an era for infrared astronomy. SOFIA was a 2.5-meter telescope carried on a Boeing 747SP aircraft whose mission was to observe the far infrared universe. In the last few years SOFIA has made some important discoveries, one of which was the detection of molecular water (H₂O) on the sunlit surface of the Moon [1, 2]. Prior to this detection it was unknown if H₂O, hydroxyl (OH) or both are responsible for the hydration signal at 3 μm . The detection and subsequent characterization of H₂O is of high interest to both the lunar and exploration communities. The instrument used to observe the Moon and detect H₂O is the Faint Object infraRed CAmera for the SOFIA Telescope (FORCAST). The spectral range of FORCAST is 5 to 8 μm which has been termed the crossover region. This region is not only home to the 6 μm H₂O feature but also to mineralogic features like olivine, pyroxene, and plagioclase [3]. This "crossover" region is new to lunar science but SOFIA's extensive observations of the Moon with FORCAST provide the only opportunity to study this spectral range currently. While SOFIA will no longer be flying in our night skies, its discoveries about the lunar water cycle and mineralogy will continue for years to come. In this abstract we present all the lunar observations conducted by SOFIA. We also provide preliminary observations of the NASA Volatiles Investigating Polar Exploration Rover (VIPER) landing region that will be used to place VIPER hydration measurements into regional context. **Observations:** At the time of writing this abstract SOFIA is still in operation conducting its final science flights in September 2022. At the end of the SOFIA mission, we will have observed the Moon on as many as 17 nights (planned nights in September can be lost to technical issues), and observations from 10 nights are currently in the SOFIA science archive. Some of observations conducted by SOFIA are spatially resolved maps of geologically important locations while others are spatially sparse maps that aim to study the behavior of H₂O across the Moon. Table 1 provides the flight names, UTC date and the target observed. All the data are or will be available on SOFIA's science archive hosted in the Infrared Science Archive (IRSA) managed by the Infrared Processing & Analysis Center (IPAC). The reduction of lunar FORCAST data is considered a special case and requires extra attention to correct for atmospheric absorption and an instrumental artifact. For further detail please refer to [1,2].

Community resources: Our team is currently working with Applied Coherent Technology to ingest SOFIA lunar observations into the Lunar Quickmap. Two products that will be available once calibrations are complete are the radiance and H₂O abundance for each pixel observed with SOFIA. Along with that supporting information such as latitude, longitude, and the lunar time of day of each pixel will be available. We are still in the beginning stages of this process.

Recent results: On February 17th, 2022 (UTC) we observed about a quarter of the lunar nearside surface south of -60° latitude with ~5 km spatial resolution. These observations covered the VIPER landing site region. After calibration and processing following procedures outlined in our upcoming paper [4] surface features are readily visible in the radiance data at 5.5 μm (Fig. 1 right). A water emission feature is observed in portions of this region and seen on the left of Fig. 1. To detect the 6 μm feature we ratio the target to a reference location ideally at higher temperatures. This means that the emission of H₂O is always with respect to a reference site. In this case the reference was Mare Fecunditatis. In this data set there is a gradual decreasing trend in H₂O toward the south pole. During these observations some of the far side was visible to SOFIA including the Nobile landing site for VIPER roughly indicated by the red circle in Fig. 1. In this image we can see H₂O features that correspond with high radiance areas but also H₂O features that do not correlate with radiance. These observations are very preliminary and in-depth analysis needs to be completed.

Upcoming investigation: With observations of the VIPER landing site and its surrounding region we will investigate the abundance of H₂O present in the region and place VIPER hydration measurements at 3 μm into regional context. The map in Fig.1 and others observed in September will allow us to estimate how much H₂O is present in on surfaces with a 3 μm hydration band detected by VIPER's Near-Infrared Volatiles Spectrometer System (NIRVSS). We have also mapped the same region with the

NASA InfraRed Telescope Facility (IRTF) at 3 μm . Comparing IRTF and VIPER results will provide a means to ground truth remote sensing data and extend the VIPER results to a broader context.

References: [1] Honniball C. I. et al. (2020) Nat Ast, 10.1038/s41550-020-01222-x. [2] Honniball C. I. et al. (2022) GRL, 10.1029/2022gl097786. [3] Kremer, C. H. et al. (2020) GRL, 47. [4] Reach W. T. et al. (in prep) Sci. Adv.

O702: Moon Rocks - Predicting lunar rock types with geochemical data using machine learning tools

Sourabh Shubham (698), Ricardo Arevalo Jr (101), Barbara Cohen (698)

Moon is composed of a suite of igneous and metamorphic rocks that vary in chemical composition, texture, and other properties. The lunar rocks have been further classified into different classes that represent different stages of lunar evolution. We can improve the age constraint of the stages of lunar magma ocean crystallization and lunar evolution timescale by performing radiometric dating of lunar rocks at different locations of the Moon. Currently, in-situ geochronology instrument suites, such as Potassium-Argon Laser Experiment (KArLE), are being developed and can perform absolute dating of lunar rocks without the need of sample return. KArLE relies on laser ablation of lunar rocks to quantify the geochemical signature of rocks through which we can quantify the major and minor oxides (in wt%) and some trace elements. In this study, we use lunar geochemical data from the analyzed samples returned from the Apollo missions and Luna missions to build a classifier through which the rock types can be identified at a potential landing sites. We test different component analysis and dimensionality reduction algorithms, such as Principal Component Analysis (PCA), Independent Component Analysis (ICA), and Linear Discriminant Analysis (LDA) to identify potential clusters for each rock type that can be expected at specific landing sites. The application of this study is to predict a lunar rock type on any future planetary mission where the major, minor, and trace elements can be quantified in lunar rocks.

O703: Composition of Comet C/2017 K2 Beyond the Water Sublimation Zone: ALMA Imaging of CO, HCN, H₂CO, and Cold CH₃OH

Nathan Roth (691), Stefanie Milam (691), Martin Cordiner (691), Charles Woodward, Nicolas Biver, Dominique Bockelee-Morvan, Jeremie Boissier, Anthony Remijan, Steven Charnley (691)

Comets afford a window into the chemistry and physics of planet formation. Through remote sensing of coma gases, the composition of nucleus ices can be inferred and placed into the context of the protoplanetary disk midplane and solar system formation. At large heliocentric distances comet activity is driven by the most volatile species, with CO sublimation beginning at heliocentric distances (rH) of up to tens of au and CO₂ sublimation activating near 6 - 8 au. Although H₂O is the dominant ice in most comets, vigorous H₂O sublimation does not begin until comets reach rH ~ 2 - 3 au in the inner solar system. The interplay between these three major drivers of cometary activity (H₂O, CO, and CO₂) across an orbit is not well understood, and the behavior of the coma as it crosses the H₂O sublimation region and transitions from CO/CO₂-driven activity to H₂O-dominated outgassing requires further study. Here we

report ALMA Cycle 8 observations of distantly active Oort cloud comet C/2017 K2 (PanSTARRS). C/2017 K2 was already active upon its discovery at 16 au, with activity consistent with CO sublimation. Its large discovery distance and high intrinsic brightness afforded an opportunity to characterize the evolution in molecular abundances, spatial distributions, and kinematics in the coma as the comet crossed the H₂O sublimation region inbound to perihelion. We monitored C/2017 K2 using ALMA beginning near rH = 4 au in 2021 January with follow-up observations in 0.5 au increments, sampling molecular emission from CO, CH₃OH, H₂CO, CS, HCN, and HNC and continuum emission from dust/icy grains as the comet approached and crossed the H₂O sublimation region. We report molecular production rates and spectrally integrated flux maps on each date, and place our results into the context of the larger comet population. This work makes use of the following ALMA data: ADS/JAO.ALMA #2021.1.00862.S.

O704: Structure-Specific Identification of Products Sublimated from UV-Photolyzed Cosmic Ice Analogues

Olivia Wilkins (691), Katarina Yocum (NPP/691), Stefanie Milam (691), Perry Gerakines (691)

Ice is prevalent throughout the solar system, from the permanently shadowed depths of Mercurian craters to icy bodies in the far reaches of the Kuiper Belt and beyond. The chemistry of these ices is influenced by several parameters, including the solar UV flux and temperature. Understanding these influences help to uncover how molecular complexity evolves from relatively simple species in the interstellar medium to prebiotic molecules that may have been delivered to the early Earth by comets and meteorites. Studying this chemistry also may help to explain the chemical diversity observed in different planetary bodies. Laboratory studies of energetically processed cosmic ice analogues have revealed a large number of chemical formation routes and require sensitive analytical techniques to identify the composition of ice and gas products formed. The unique identification of organic species can be challenging and often requires structure-specific techniques to identify structural isomers, conformers, and isotopologues. The Sublimation Laboratory Ice Millimeter/submillimeter Experiment (SubLIME) explores cometary and planetary ice chemistry with the structure-specificity of rotational spectroscopy to identify and measure the abundance ratios of products sublimated from UV-photolyzed ices. Samples are formed at low temperature (~10 K) and photolyzed at temperatures relevant to planetary bodies. After photolysis, the samples are slowly heated to 300 K to sublimate the volatile products, the gas mixture of which is then analyzed with (sub)millimeter spectroscopy. We present the experimental setup and research projects of SubLIME, including results of UV-photolyzed ice analogues containing water (H₂O) and carbon monoxide (CO) and previous findings of methanol (CH₃OH) photolysis. Additionally, new work on mixed ices provokes interesting new species not necessarily detectable with other techniques. Experimental results and current projects are discussed in the context of observations of comets and other planetary bodies.

O705: Life Detection Knowledge Base: Organizing Astrobiology Knowledge for Mission Development and Calling for Contributors

Svetlana Shkolyar (698), S. Shkolyar (698/UMCP), T. M. Hoehler, R. C. Quinn, A. Pohorille, L. E. Bebout, W. B. Brinckerhoff (690), A. F. Davila, D. Des Marais, S. Getty (690), L. Jahnke, G. Lau, O. Lehmer, M. Neveu (699/UMCP), M. N. Parenteau, A.C. Rios, S. Som, M. B. Wilhelm

Life detection mission development is based on a body of knowledge that is often diverse (taking forms that do not map clearly to mission requirements) and diffuse (spread across many disciplines and literature fields lying beyond the traditional sphere of space sciences). A suite of web tools, the Life Detection Forum (LDF), is currently being built to capture and organize this evolving body of knowledge, to streamline its utilization in mission science development, and to aid in establishing science traceability to current and emerging measurement technologies. The primary and most developed tool of the suite is the Life Detection Knowledge Base (LDKB), which will be the emphasis of this talk. These tools are being built by members of the NASA Network for Life Detection (NfoLD) Center for Life Detection, an ARC-GSFC collaboration with support from PSD/ISFM. Still, they rely heavily upon engagement activities that enable members of the broader astrobiology community to provide ongoing input into their formulation. Technologists and researchers are invited to learn about the LDKB's evolution, current state, and upcoming development plans, as well as how they can contribute their expertise to the tool in numerous ways (including amplifying their research publications, adding new biosignature content, providing content reviews, and participating in upcoming community workshops).

O706: The Transformation and Export of Organic Carbon Across an Arctic River-Delta-Ocean Continuum

J. Blake Clark (616), Antonio Mannino (616), Maria Tzortziou, Robert G.M. Spencer, and Peter Hernes

The Arctic Ocean is surrounded by land masses that feed highly seasonal rivers with waters enriched in relatively high concentrations of dissolved and particulate organic carbon (DOC and POC). Explicit estimates of the flux of organic carbon across the land-ocean interface are difficult to quantify and many interdependent processes makes source attribution difficult. A high-resolution 3-D biogeochemical model was built for the lower Yukon River and coastal ocean to estimate biogeochemical cycling across the land-ocean continuum. The model solves for complex reactions related to organic carbon transformation, including mechanistic photodegradation and multi-reactivity microbial processing, DOC to POC flocculation, and phytoplankton dynamics. The baseline DOC and POC flux out of the delta from April to September 2019, was 977 and 536 Gg C, respectively, making up ~80% of the annual total, but only 50% of the DOC and 25% of the POC exited the plume across the 10 m isobath. Microbial breakdown of DOC accounted for a net loss of 168 Gg C (17% of delta export) within the plume and photodegradation accounted for a net loss of 46.6 Gg C DOC (4.7% of delta export) in 2019. Flocculation decreased the total organic carbon flux by only 6.4 Gg C (~1%), while POC sinking accounted for 63.3 Gg C (10%) settling in the plume. The loss of CDOM due to photodegradation increased the light available for phytoplankton growth throughout the coastal ocean, demonstrating the secondary effects that organic carbon reactions can have on biological processes and the net coastal carbon flux.